

Adatom-Adatom Interaction Mediated by an Underlying Surface Phase Transition

I. Brihuega, A. Cano,^{*} M. M. Ugeda, J. J. Sáenz, A. P. Levanyuk, and J. M. Gómez-Rodríguez[†]

Departamento de Física de la Materia Condensada, Universidad Autónoma de Madrid, E-28049 Madrid, Spain

(Received 18 May 2006; published 13 April 2007)

Low temperature scanning tunneling microscopy measurements on the adsorption of single Pb adatoms on Si(111)-($\sqrt{3} \times \sqrt{3}$)-Pb surfaces reveal the vertical displacement patterns induced on the substrate by these Pb adatoms as well as a novel adatom-adatom interaction. The origin of both can be traced back to the ($\sqrt{3} \times \sqrt{3}$) \leftrightarrow (3×3) phase transition taking place at lower temperatures. A Landau-like approach explains the displacement patterns as due to the corresponding order parameter and shows that the vicinity of a surface phase transition gives rise to a nonmonotonic adatom-adatom interaction.

DOI: [10.1103/PhysRevLett.98.156102](https://doi.org/10.1103/PhysRevLett.98.156102)

PACS numbers: 68.35.Rh, 68.37.Ef, 68.43.Jk

Substrate-mediated interactions between adsorbed atoms play a key role in determining the static and dynamic properties of surfaces. Understanding these interactions is of high interest in a large variety of fundamental and technological problems ranging from epitaxial growth to heterogeneous catalysis. A considerable experimental effort has been made towards measuring adatom-adatom interactions, early on by field ion microscopy [1–3] and much more recently by scanning tunneling microscopy (STM) [4–9]. These interactions have usually been associated with the adatom coupling with the substrate elastic [10] or electronic [11–13] degrees of freedom. The coupling with the additional degrees of freedom behind a phase transition in the substrate could provide a significant new contribution to the adatom-adatom interaction.

In this Letter we present theoretical and experimental results showing the existence of an interaction between adatoms mediated by an underlying surface phase transition. The interaction results from the system softening at wave vectors close to those associated with the corresponding order parameter of the transition, i.e., via the corresponding “soft phonon.” This new interaction differs from all other previously discussed in being a temperature dependent “tunable” interaction: the closer the transition is, the more important the interaction should become. Here we present a detailed STM study of the adsorption of small amounts of additional Pb adatoms on top of the clean Si(111)-($\sqrt{3} \times \sqrt{3}$)R30°-Pb surface ($\sqrt{3}$ in the following) and show that, in fact, the above interaction, associated to the $\sqrt{3} \leftrightarrow (3 \times 3)$ phase transition [14,15], takes place. This can be considered as an example of the interaction between defects close to structural phase transitions [16]. In this context, our results provide the first direct observation of such an interaction in the case of a two-component order parameter and defects with internal structure.

Our STM study reveals that the adsorption of single additional Pb adatoms on the $\sqrt{3}$ surface of the Pb/Si(111) system induce, at temperatures well below room temperature (RT) but above $T_c \sim 86$ K [15], a long range perturbation on the substrate atoms whose symmetry can be unambiguously related to the low temperature (LT)

(3×3) phase. It is worth mentioning that the phase transition in our system is related to those observed in the isoelectronic Pb/Ge(111) [17] and Sn/Ge(111) [18] systems, whose origin and driving force have been the subject of an intense debate, where the role of the intrinsic substitutional defects has not been absent [18–20]. Our theoretical analysis of the displacement patterns on the Pb/Si(111) surface shows that the main contribution comes from the soft phonon of the phase transition. According to this it is reasonable to expect the existence of some adatom-adatom interaction related to the soft phonon. We show that, indeed, a novel nonmonotonic adatom-adatom interaction mediated by the underlying phase transition can be detected in the present case by comparing thorough quantitative STM measurements of the pair interactions between the additional Pb adatoms with theoretical interaction maps based on the soft-phonon contribution.

The experiments were carried out in an ultrahigh vacuum system equipped with a home-built variable temperature STM [21,22]. The sample preparation starts by growing exceptionally large domains of the $\sqrt{3}$ reconstruction as described in Ref. [15]. Then, additional Pb atoms (~ 0.005 ML) were deposited on these $\sqrt{3}$ surfaces while maintaining the sample temperature below 140 K. This procedure results in isolated Pb single adatoms adsorbed on the $\sqrt{3}$ reconstruction.

Figure 1(a) shows a large scale STM image of single Pb adatoms on the $\sqrt{3}$ surface at 140 K. Besides a ($\sqrt{7} \times \sqrt{3}$) island [23] on the left part, a very large and perfect domain of the $\sqrt{3}$ reconstruction can be observed where some triangular features are resolved. These features can be ascribed to the adsorption of additional single Pb adatoms on top of the $\sqrt{3}$ surface. For temperatures above ~ 145 K these single adatoms start to diffuse to neighboring sites at frequencies accessible to STM. Temperature dependent measurements, performed by means of STM movies on samples with lower concentration of additional Pb adatoms, have allowed to measure the diffusion barrier ($E_d = 0.45 \pm 0.01$ eV) and the attempt frequency ($\nu_0 = 10^{13.0 \pm 0.4}$ Hz) [24].

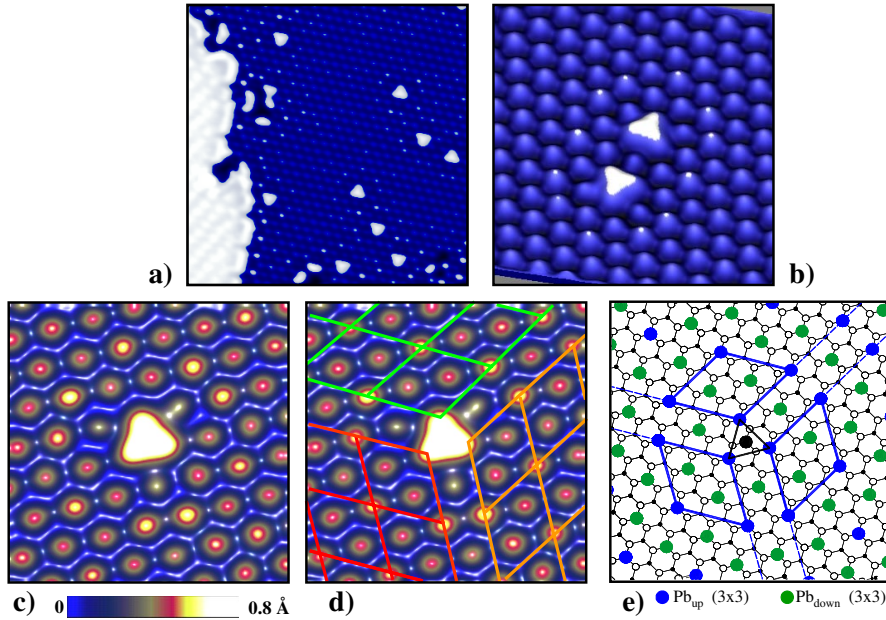


FIG. 1 (color online). (a) STM image of single Pb adatoms adsorbed on the $\sqrt{3}$ -Pb/Si(111) surface. (b) and (c) STM images showing substrate displacement patterns induced by two Pb adatoms (b) and by a single one (c). (d) same image as (c) with 3 translational domains of the LT (3×3) reconstruction superimposed. A schematic atomic model for the modified $\sqrt{3}$ surface is shown in (e). The STM image sizes, sample voltages, tunnel currents, and measurement temperatures are (a) $18 \times 18 \text{ nm}^2$, -0.5 V , 0.1 nA , 140 K ; (b) $7 \times 7.6 \text{ nm}^2$, -0.5 V , 0.1 nA , 150 K ; (c) $4.5 \times 4.5 \text{ nm}^2$, -0.5 V , 0.1 nA , 150 K .

A remarkable feature of Fig. 1(a) is that, around each Pb extra adatom, the substrate presents regular patterns of apparent vertical displacements. These patterns are strongly affected by the presence of neighboring extra adatoms. This can be very nicely seen in Fig. 1(b), where the patterns associated with two close extra adatoms seem to interact and form a new complex displacement pattern whose form strongly depends on the relative orientations of the adatoms. In order to elucidate the origin of such perturbations, we first analyze the pattern for a single isolated adatom. Figures 1(c)–1(e) show that there are nine substrate atoms around the central triangular feature (corresponding to the additional adatom and three substrate atoms) that present a higher contrast (i.e., apparent vertical height) than the others. As sketched in (d) and (e), this pattern can be rationalized as the stabilization of three different translational domains of the LT and low symmetry (3×3) phase.

In the following we show that these displacement patterns can be explained as due to the softening of the system at wave vectors close to those associated with the order parameter that, in our case, corresponds to spontaneous displacements modulated with the wave vectors \mathbf{k}_α shown in Fig. 2(a) [15,25]. Let $u(\mathbf{r})$ be the function describing the transversal displacements in the system. This function can be expressed as $u(\mathbf{r}) = \sum_{\mathbf{k}} q_{\mathbf{k}} e^{i\mathbf{k}\cdot\mathbf{r}}$, where the wave vectors \mathbf{k} are within the surface first Brillouin zone (SBZ). The free energy of the system can be written phenomenologically in terms of the magnitudes $q_{\mathbf{k}}$ as $\Phi = \Phi_0 + \frac{1}{2} \sum_{\mathbf{k}} \Lambda(\mathbf{k}) |q_{\mathbf{k}}|^2 + \dots$, where $\Lambda(\mathbf{k})$ determines the stiffness associated to displacements patterns modulated with \mathbf{k} . Consequently, the softening of the system that finally gives rise to the phase transition implies that $\Lambda(\mathbf{k})$ has local minima at \mathbf{k}_α that virtually drop to zero at the transition point.

The presence of an additional Pb adatom on the $\sqrt{3}$ phase of Pb/Si(111) can be modeled as three point forces

of the same strength acting on its three nearest neighbors: $F(\mathbf{r}) = f \sum_{i=1}^3 \delta(\mathbf{r} - \mathbf{r}_i)$ (see Fig. 1). Taking into account these forces, the free energy reads

$$\Phi = \Phi_0 + \frac{1}{2} \sum_{\mathbf{k}} \Lambda(\mathbf{k}) |q_{\mathbf{k}}|^2 - \sum_{\mathbf{k}} F_{\mathbf{k}} q_{-\mathbf{k}} \quad (1)$$

in the harmonic approximation, where $F_{\mathbf{k}} = f \sum_{i=1}^3 e^{-i\mathbf{k}\cdot\mathbf{r}_i}$. The equilibrium value of the normal coordinates and the corresponding value of the free energy can be obtained by minimizing (1). The presence of adatoms gives rise to nonvanishing equilibrium displacements even in the symmetric phase:

$$u^{(\text{eq})} = \sum_{\mathbf{k}} \frac{F_{\mathbf{k}}}{\Lambda(\mathbf{k})} e^{i\mathbf{k}\cdot\mathbf{r}} = f \sum_{i=1}^3 \sum_{\mathbf{k}} \frac{e^{i\mathbf{k}\cdot(\mathbf{r}-\mathbf{r}_i)}}{\Lambda(\mathbf{k})}. \quad (2)$$

The contribution to these displacements due to wave vectors $\mathbf{k} \approx \mathbf{k}_\alpha$ increases as the phase transition is approached and $\Lambda(\mathbf{k}_\alpha)$ tends to zero. This is just the contribution due to the “soft” normal coordinates, or soft phonon, of the transition. To find out this contribution, we expand $\Lambda(\mathbf{k})$ in a power series about \mathbf{k}_α and retain the lowest order terms: $\Lambda(\mathbf{k}) \approx A + D(\mathbf{k} - \mathbf{k}_\alpha)^2$. The aforementioned vanishing of $\Lambda(\mathbf{k}_\alpha)$ at the transition point implies that the magnitude $\xi = \sqrt{D/A}$ diverges at this point (ξ can be understood as the corresponding correlation length). In view of this, close to the transition point we can replace $\Lambda(\mathbf{k})$ in (2) by the above expansion and take the continuous medium limit in further calculations (i.e., extend sums up to infinity) without altering the overall result significantly. Replacing sums by integrals, the soft-phonon-mediated displacements due to the presence of the additional Pb adatom is found

$$u_{\text{s-ph}}^{(\text{eq})} = \frac{f}{3\pi D} \sum_{i=1}^3 \sum_{\alpha=1}^3 K_0(|\mathbf{r} - \mathbf{r}_i|/\xi) \cos[\mathbf{k}_\alpha \cdot (\mathbf{r} - \mathbf{r}_i)], \quad (3)$$

where K_0 is the McDonald function.

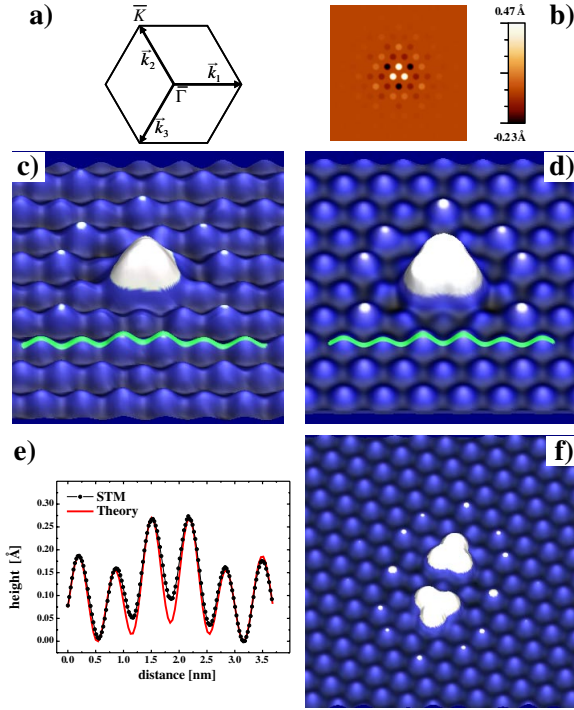


FIG. 2 (color online). (a) SBZ of the $\sqrt{3}$ surface including \mathbf{k}_α of soft phonons. (b) Theoretical displacement pattern calculated using (3) with $\xi = 7 \text{ \AA}$ and $f/D = 2.6 \text{ \AA}$. Experimental (c) and simulated (d) STM images of an additional Pb adatom adsorbed on the $\sqrt{3}$ -Pb/Si(111) surface. The experimental image ($5 \times 5 \text{ nm}^2$) was measured at 150 K, at a sample bias of -1.5 V and a tunnel current of 0.1 nA . (e) Experimental and theoretical profiles across the lines shown in (c) and (d). (f) Theoretical image illustrating the displacement pattern corresponding to two close Pb adatoms as those shown in the experimental image in Fig. 1(b).

Figure 2(b) shows the soft-phonon-induced displacement pattern calculated according to (3) with $\xi = 7 \text{ \AA}$ and $f/D = 2.6 \text{ \AA}$. This pattern accurately reproduces the experimental measurements shown in Fig. 1: the formation of three translational domains of the LT (3×3) phase with decaying amplitude. In Figs. 2(c) and 2(d) a comparison of experimental and theoretical STM images [calculated by adding the pattern in (b) to a $\sqrt{3}$ simulated image] are displayed. The agreement between experiments and theory is excellent even in its more subtle details as can be observed in the profiles shown in (e). Also, the more complex patterns measured when two additional adatoms are in close proximity are well explained by the theory [compare Figs. 1(b) and 2(f)]. This makes it reasonable to expect that there is a significant interaction between these adatoms due to the existence of the soft phonon which could be detectable even for a relatively small correlation length.

In order to test quantitatively the existence of this new kind of adatom-adatom interaction, extended STM experiments were performed. Regions with only two isolated adatoms were selected where any other defect was more

than 40 \AA away. Then, very long STM movies were measured at 150 K [26] and the relative positions of the pair of adatoms were recorded. Figure 3(a) displays some frames of such kinds of movies where 6 nonequivalent relative positions of two interacting adatoms are shown. The total time corresponding to each of the 24 nonequivalent positions shown in (b) were measured and a histogram was drawn accordingly as shown in (c). From it, it is straightforward to calculate the interaction energy (ΔE_{int}) as a function of the relative adatom-adatom position (\mathbf{r}) using Boltzmann statistics as $\Delta E_{\text{int}} = -k_B T \ln[W(\mathbf{r})/W_{\text{ran}}(\mathbf{r})]$, where $W(\mathbf{r})$ is the experimental probability at a given position obtained from the histogram shown in Fig. 3 and $W_{\text{ran}}(\mathbf{r})$ is the probability corresponding to two non-interacting adatoms, obtained from a simple Monte Carlo simulation in order to take into account finite size effects (similar to [2,6,7]) in the STM images. Figure 4(a) shows the experimental interaction map obtained in that way. This map reflects that the interaction energy depends not only on the distance but also on the relative orientation of the pair of adatoms in a nonmonotonic way.

The soft-phonon contribution to the free energy can be calculated in the same way as the displacement patterns. Under the same assumptions as those used for deducing (3) one finds that the interaction energy is

$$\Phi_{\text{s-ph}}^{(\text{eq})} = -\frac{f^2}{3\pi D} \sum_{i,j=1}^3 \sum_{\alpha=1}^3 K_0(R_{ij}/\xi) \cos(\mathbf{k}_\alpha \cdot \mathbf{R}_{ij}), \quad (4)$$

where $\mathbf{R}_{ij} = \mathbf{r} \pm (\mathbf{r}_i - \mathbf{r}_j)$, with $+$ for two adatoms on the same and $-$ for those on different $\sqrt{3}$ sublattices [27].

Figure 4(b) shows the theoretical interaction map calculated according to (4) and using $\xi = 7 \text{ \AA}$, i.e., the correla-

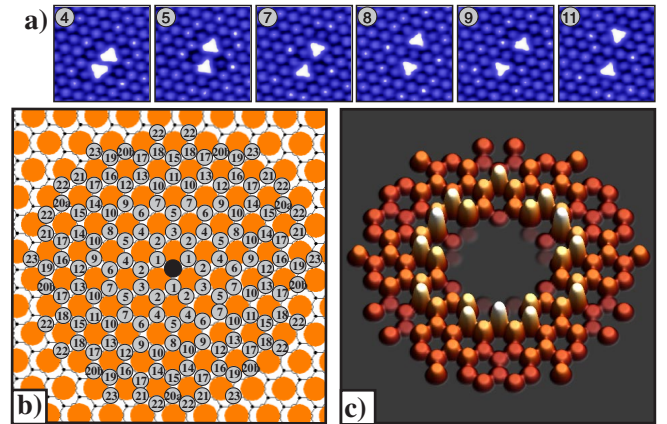


FIG. 3 (color online). (a) STM images extracted from a movie showing six nonequivalent relative positions of a pair of Pb adatoms (sample bias -0.5 V and tunnel current 0.1 nA). (b) Schematic drawing displaying the 24 relative positions measured. They correspond to adatom-adatom distances up to 30 \AA . (c) Experimental histogram corresponding to the diagram shown in (b). The total time of the measurement corresponds to 35000 s and the maximum peak represents 1600 s . Positions from 1 to 3 were never observed in the measurements and are not displayed in (c).

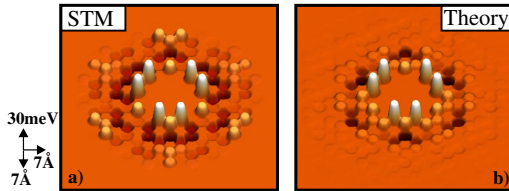


FIG. 4 (color online). Comparison of experimental (a) and theoretical (b) interaction maps for a pair of Pb adatoms. The experimental vertical scale ranges from a maximum of +29 meV (repulsive interaction) to a minimum of -15 meV (attractive interaction). Both maps correspond to the same area as Fig. 3(c) (7×7 nm²). A three-dimensional scale common to both maps is shown on the left.

tion length obtained from the displacement patterns as a fitting parameter, and $f^2/D = 0.3$ eV [28,29]. A comparison between experimental and theoretical maps reveals (i) that both interaction maps present an oscillatory character along the three equivalent $\langle 1\bar{1}0 \rangle$ directions (i.e., the 3×3 directions) and (ii) that there is a reasonable agreement between both maps for distances up to $r \leq 2\xi = 14$ Å, i.e., the same range of distances for which the displacement pattern is significant [see Fig. 2(b)]. Some discrepancies, however, exist between experiment and theory for longer distances. The origin of the long range behavior of the experimental map is not clear at present. It is quite plausible, however, that a remaining substrate-mediated electronic interaction [6,7] could dominate at larger distances due to the limited correlation length corresponding to the actual experimental temperature. The importance of the soft-phonon contribution should increase at temperatures closer to the transition temperature, as long as the correlation length virtually diverges there. So, in principle, such a contribution could be enhanced by measuring an interaction map at lower temperatures. When lowering the temperature, however, Pb adatoms freeze up, making it impossible to obtain that map in this particular system by STM.

In summary, by combining quantitative STM measurements on the adsorption and interaction of pairs of single adatoms on a $\sqrt{3}$ -Pb/Si(111) surface at temperatures relatively close to an underlying phase transition with a (phenomenological) Landau-type analysis, we have been able to detect and understand the contribution of the soft phonon of the phase transition to both the surface displacement patterns surrounding isolated adatoms and the interaction between them at moderate distances. Our prediction that this new soft phonon contribution to the adatom-adatom interaction should be the leading term, overwhelming any other, at temperatures very close to the transition is an exciting challenge for further experimental research of adatom-adatom interactions on other surfaces undergoing structural phase transitions.

This work was supported by Spain's MEC under Grants No. MAT2004-03129 and No. NAN2004-09183-C10-05.

*Present address: Instituto de Astrofísica de Andalucía (CSIC), P.O. Box 3004, E-18080 Granada, Spain.

†Corresponding author.

Electronic address: josem.gomez@uam.es

- [1] H. W. Fink, K. Faulian, and E. Bauer, Phys. Rev. Lett. **44**, 1008 (1980).
- [2] T. T. Tsong and R. Casanova, Phys. Rev. B **24**, 3063 (1981).
- [3] F. Watanabe and G. Ehrlich, Phys. Rev. Lett. **62**, 1146 (1989).
- [4] J. Trost *et al.*, Phys. Rev. B **54**, 17 850 (1996).
- [5] L. Österlund *et al.*, Phys. Rev. Lett. **83**, 4812 (1999).
- [6] J. Repp *et al.*, Phys. Rev. Lett. **85**, 2981 (2000).
- [7] N. Knorr *et al.*, Phys. Rev. B **65**, 115420 (2002).
- [8] T. Mitsui *et al.*, Phys. Rev. Lett. **94**, 036101 (2005).
- [9] I. Ošt'ádal *et al.*, Phys. Rev. Lett. **95**, 146101 (2005).
- [10] K. H. Lau and W. Kohn, Surf. Sci. **65**, 607 (1977).
- [11] T. B. Grimley, Proc. Phys. Soc. London **90**, 751 (1967).
- [12] T. L. Einstein and J. R. Schrieffer, Phys. Rev. B **7**, 3629 (1973).
- [13] K. H. Lau and W. Kohn, Surf. Sci. **75**, 69 (1978).
- [14] O. Custance *et al.*, Surf. Sci. **482–485**, 1399 (2001).
- [15] I. Brihuega *et al.*, Phys. Rev. Lett. **94**, 046101 (2005).
- [16] H. Schmidt and F. Schwabl, Phys. Lett. A **61**, 476 (1977); A. P. Levanyuk and A. S. Sigov, *Defects and Structural Phase Transitions* (Gordon & Breach, New York, 1987).
- [17] J. M. Carpinelli *et al.*, Nature (London) **381**, 398 (1996).
- [18] L. Petersen, Ismail, and E. W. Plummer, Prog. Surf. Sci. **71**, 1 (2002); J. Ortega, R. Pérez, and F. Flores, J. Phys. Condens. Matter **14**, 5979 (2002), and references therein.
- [19] A. V. Melechko *et al.*, Phys. Rev. B **61**, 2235 (2000).
- [20] I. Brihuega *et al.*, Phys. Rev. Lett. **95**, 206102 (2005).
- [21] O. Custance *et al.*, Phys. Rev. B **67**, 235410 (2003).
- [22] STM data acquired and processed with WSxM. See I. Horcas *et al.*, Rev. Sci. Instrum. **78**, 013705 (2007).
- [23] J. Slezák, P. Mutombo, and V. Cháb, Phys. Rev. B **60**, 13 328 (1999); S. Brochard *et al.*, *ibid.* **66**, 205403 (2002).
- [24] I. Brihuega, M. M. Ugeda, and J. M. Gómez-Rodríguez (to be published).
- [25] R. Pérez, J. Ortega, and F. Flores, Phys. Rev. Lett. **86**, 4891 (2001); D. Fariás *et al.*, *ibid.* **91**, 016103 (2003).
- [26] At this temperature adatoms diffuse in a large enough region that still allows the measurement of STM images at reasonable rates (typically 10 s/frame).
- [27] Pb adatoms can occupy two different sites of a honeycomb lattice with $\sqrt{3}$ periodicity (see Fig. 3).
- [28] Pb adatoms share nearest neighbors at positions 1 to 3. Equation (4) cannot be applied for these positions and, consequently, they are not drawn in Fig. 4.
- [29] From the comparison of experimental and theoretical data both for the displacements and the interaction energies we find that $f = 0.1$ eV/Å and $D = 0.04$ eV/Å². Very general arguments for structural phase transitions [see, e.g., V. G. Vaks, Sov. Phys. JETP **27**, 486 (1968)] indicate that these parameters can be roughly estimated as $f \sim \alpha E_{\text{at}}/d$ and $D \sim E_{\text{at}}/d^2$, where E_{at} is an atomic energy, d represents an atomic distance, and α is a numerical coefficient indicating whether Pb adatoms can be considered as strong defects or weak ones. The order of magnitude of our parameters f and D is in tune with these estimates.